International Journal of Engineering Works
https://www.ijew.io/
ISSN-p: 2521-2419
ISSN-e: 2409-2770
Vol. 10, Issue 06 PP. 55-63, June 2023
https://doi.org/10.34259/ijew.23.10065563

Using Computer Tomographic (CT) Images, A Rebust Hybrid Computer-Aided Deep Learning Framework for Lung Cancer Classification

Abdul Jabbar*, M. Irfan Khtaak, Arif ULLAH
University of Engineering & Technology, Peshawar
abduljabbar-msece@uetpeshawar.edu.pk*
Received: 20 May, Revised: 10 June, Accepted: 12 June

***Abstract*—**Various forms of cancer have been recognized, all sharing a common objective: the rapid destruction of healthy tissue. To enhance a patient's chances of surviving cancer, it is crucial to accurately diagnose and prognose the specific type of underlying disease. Early identification and personalized treatment can potentially improve survival rates. Additionally, it is important to differentiate cancer patients based on their risk levels for disease progression. In the past, data mining and machine learning algorithms have been employed for cancer diagnosis. However, these approaches rely on manually conducted feature extraction techniques, resulting in unreliable categorization. Consequently, precise cancer identification becomes a time-consuming task fraught with the possibility of pathologist errors. In contrast, deep learning has recently gained significant traction in categorization and detection fields, owing to its powerful feature extraction capabilities. Therefore, I utilized a hybrid deep learning model to achieve better accuracy in identifying cases of lung cancer.

***Keywords*—** Deep learning, hybrid models, machine leaning, cancerous.

I. INTRODUCTION

Several Lung cancer possesses the highest fatality rate among all cancer types, prompting numerous countries to develop tools for early detection of the disease. Extensive studies like the NLST [1,2] have shown that screening high-risk individuals three times a year using low-dose computed tomography (CT) significantly reduces mortality rates. Consequently, radiologists face the challenge of reviewing a substantial number of CT scan images resulting from these screenings. Even experienced doctors find it difficult to identify lesions, placing increasing pressure on radiologists. The lungs, situated in the thoracic cavity, are vital for human respiration. When normal lung cells undergo malignant transformation, lung cancer develops, causing the demise of approximately 27% of cancer patients [1]. Mutations, alterations in DNA sequences, can be caused by environmental factors or inherited genetic defects, leading to uncontrolled cell proliferation. While chemicals in cigarette smoke are well-known environmental carcinogens, other factors can also contribute. Normally, damaged tissue is replaced with fresh tissue, but when cancer-causing mutations occur, new tissue grows uncontrollably, resulting in the formation of malignant cells. Although the majority of lung nodules are harmless, some may indicate precancerous conditions (suspicious nodules). Recent research indicates a discouraging 5-year survival rate of 19% for lung cancer patients [2]. Early-stage diagnosis plays a crucial role in improving survival rates, as with many other cancers. Unlike cancerous tumors, benign nodules do not spread to other parts of the body. The World Health Organization (WHO) predicts that cancer will become the leading cause of global mortality by 2030 [3].

Lung cancer ranks as the second most prevalent malignancy leading to mortality. While over 80% of individuals diagnosed with bladder, breast, colon, cervical, and prostate cancer survive for five years or more, early identification of lung cancer is crucial to reduce death rates and facilitate effective treatment. Early-stage lung malignancies and pre-cancerous conditions such as dysplasia and carcinoma in situ (CIS) can be visually challenging to detect due to their thin cell layers (0.1-2 mm) and lack of symptoms, making traditional diagnostic methods like medical imaging less effective. In clinical practice, around 80% of cases are diagnosed at advanced stages, missing the best opportunity for surgical intervention. From a medical perspective, early diagnosis of lung cancer is crucial. An important morphological characteristic of malignant cells is an atypical shape and size of the nucleus [4]. CT image morphology is often used to differentiate between benign and cancerous nodules. Currently, the expertise of highly trained radiologists plays a primary role in determining whether a tumor is benign or malignant. However, forming a conclusive opinion can be challenging when everything appears proportionate. Morphological data is employed to train

classifiers that automatically distinguish between benign and malignant nodules. Utilizing additional characteristics helps overcome subjectivity issues, and classification can be achieved using single or multiple classifiers in conjunction with other information [5]. Detecting nodules in their early stages significantly improves a patient's prognosis. Therefore, the identification of potentially cancerous nodules in the lungs is essential for lung cancer diagnosis. Comparing the characteristics of benign and malignant nodules is a reliable method for identifying lung cancer [6]. Due to the overlapping characteristics of benign and malignant nodules, rigorous morphological evaluation is necessary for accurate nodule assessment, as prompt and accurate diagnosis is crucial [7].

To alleviate physician workload, enhance diagnostic accuracy, expedite procedures, and reduce subjectivity, automated solutions are being developed in anticipation of increased monitoring and preventive measures. Determining whether cells are cancerous relies on recognizing and assessing defining traits. The likelihood of cancer can be determined based on these identified features and their combination. However, differentiating between nodules and a positive cancer diagnosis is a challenging task, even for experienced medical professionals. Qualities such as volume, shape, subtlety, stiffness, assumption, sphericity, among others, are frequently used in computer-assisted diagnostic (CAD) techniques. Computed tomography (CT) scans are valuable in detecting potentially problematic nodules at an early stage. These scans provide detailed information about bones, soft tissues, and blood vessels compared to standard X-rays, leading to their increased usage. However, due to the similarity between lung nodules and surrounding structures, CT scans performed as part of early-stage lung cancer screening sometimes fail to detect them (e.g., blood vessels). Hence, there is a critical need to develop a CAD system specifically designed for identifying potentially harmful nodules. Deep learning has emerged as a promising area of research for separating benign and dangerous cancerous nodules, as it can reduce the number of imaging tests required to determine nodule characteristics and improve accuracy [8]. By employing cutting-edge deep learning algorithms, the CAD system can accurately classify lung nodules, identifying potentially malignant tumors and assessing their impact on a person's health.

In the task of determining whether nodules are cancerous, machine learning technologies such as Support Vector Machine (SVM) are utilized by doctors. Although widely employed [3-10], machine learning frameworks require substantial customization to achieve optimal results, as there is no standardization in CT scanners used for screenings, posing a significant risk. Deep learning, through extensive training, can prioritize and acquire crucial characteristics, enabling end-to-end identification using CAD systems. The learning process enables the network to be robust to data variations by integrating tumor data from multiple CT scans using recurrent modes. If the training dataset encompasses sufficient variations, the system can learn invariant properties of malignant nodules independently, leading to improved results [11,12]. This facilitates the growth of the system, as there are no heritable characteristics, and the network should be capable of deducing the relationship between personal traits and the respective disease from the available data. The ability of the network to generalize its training to novel situations is crucial for accurately identifying malignant tumors or cancerous regions alongside medical beds [13,14]. Figure 1.1 illustrates normative and atypical CT scans of the lungs [15]. Categorizing lung cancer and detecting the disease at an early stage are essential steps in developing an intelligent and reliable diagnostic system. Support Vector Machines (SVM), Naive Bayes Classifiers (NB), Ensemble Classifiers (EC), Artificial Neural Networks (ANN), and other common machine learning algorithms are employed for early identification of lung tumors [16]. Deep learning has shown great promise in advancing medical imaging and diagnostics [17].

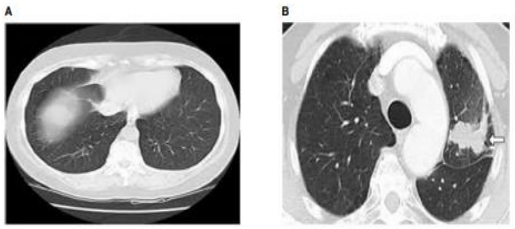

Figure 1.1: (A) Lung Image (CT) (Normal) (B) Lung Image (CT) (Abnormal). [17]

Despite the effectiveness of CAD systems in detecting lung nodules, few studies have taken into account the typical procedures followed by radiologists. Radiologists often analyze Maximum Projection Intensity (MIP) images to locate potential nodular lesions for diagnostic purposes. MIP enhances the visibility of nodules by projecting the intensity from three-dimensional voxels onto the projection plane, resulting in increased detectability [18].

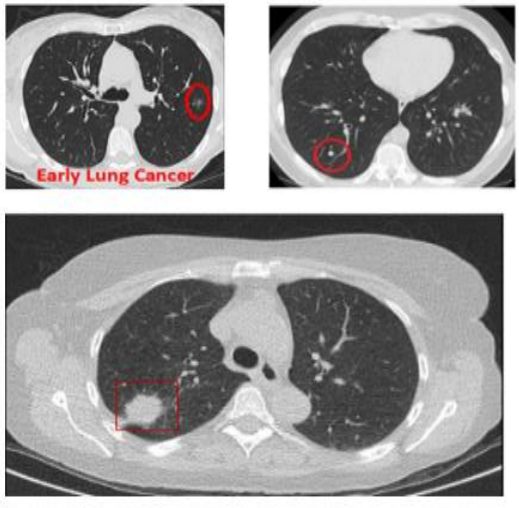

Figure 1.2: Based on maximum intensity projection CT image. [19]

Since MIP images are not reliant on specific thresholds and retain attenuation information, Convolutional Neural Networks (CNN) are well-suited for automated identification of lung nodules [19]. Figure 1.2 illustrates CT scans depicting cases of lung cancer in their early stages, encompassing both malignant and benign lung tumors. Currently, it is challenging to distinguish vascular and malignant nodules. The disease is easiest to identify in its advanced stages when nodules are larger, but prognosis for the patient is typically poor.

However, training learning models for improved performance remains challenging due to the diverse range of imaging techniques utilized in the images. To address this issue, a new hybrid intelligent diagnostic framework called the Deep hybrid DenseNet201-GRU model is introduced in this study. The framework combines saliency maps and convolutional layers within the DenseNet201-GRU architecture to enhance segmentation and feature extraction. The training process involves utilizing ant-lion optimization to train single feed-forward networks. This study is believed to be the first to integrate fused characteristics with optimized learning networks, resulting in a robust CT-based lung cancer diagnostic tool. The researchers involved in this project developed these networks.

II. Related Work

De Bruijne [21] employed this framework to assess novel techniques for lung cancer detection and diagnosis. Advanced algorithms for lesion detection, identification, and classification have been refined using labeled datasets like LIDC-IDRI, LUNA 16, and Super Bowl Dataset 2016. Jindal et al. [22] established these datasets as the standard minimum threshold CT data required for analysis. Nalepa and Kawulok [23] devised a modified-CNN to detect lung cancer cells in segmented images. The ACM technique, initially used for tumor division, can now identify cancerous cells amidst healthy ones. Label-free methods preserve cellular properties and structure. This research merged cutting-edge Prony techniques and optical coherence tomography to enhance cell identification using captured optical profiles. Ganesan et al. [24] improved the Tobacco Exposure Pattern (TEP) prediction model, identifying signature genes and their interconnectedness across biological levels. Kasinathan et al. [25] introduced the novel TTZ technique for data collection, informing TEP categorization. The TEP classification model achieved 91.85% accuracy for validation data and 94.65% for training data using separate LUAD datasets, discovering 34 genes linked to nicotine-related mutation signatures.

The author differentiated between five categories of lung and colorectal tissues (two benign and three malignant) using tissue samples, achieving a 96.33% sensitivity in tumor cell detection [26]. Suzuki's framework [27] outlines the procedures for determining EGFR mutation status using CA-diagnostics, including data collection, analysis, and integration of multi-type dependence characteristics. The research utilized a unique hybrid CNN-RNN network model, extracting quantitative image properties and modeling feature interdependence. Multi-type dependency-based feature representations outperformed conventional approaches, achieving an accuracy of 75% and an AUC of 0.78.

The 3D Alex Net, an unsupervised learning model, was introduced for lung cancer diagnosis [28]. Its 3D CNN architecture enhances tumor visibility and prediction accuracy. Fang [40] employed MIP to automatically identify lung cancer-related nodules from CT scans at various angles. Drokin et al. [41] presented a comprehensive technique for detecting worrisome lung nodules using CNN-type MIP images in the form of U-Net. Eman et al. [42] successfully distinguished lungs from CT images using histogram, thresholding, and morphological approaches. Various methods such as neuro-fuzzy algorithms, SVM-based classification, and watershed segmentation were utilized for lung nodule identification and classification [43-46]. Chon et al. proposed a multi-crop convolutional neural network to remove nodules from CT scans, aiming to improve cancer detection rates [47]. Ding et al. proposed Fast RCNN for nodule extraction from CT scans, achieving a 94% sensitivity [49]. Zhu et al. introduced F-CNN, a three-dimensional network, achieving a 90.44% accuracy on the LUNA16 dataset [50]. Shakeel et al. employed a weighted mean histogram equalization method, obtaining a 98.42% accuracy with DITNN [52]. Different CNN models and techniques were applied for classifying lung nodules [53-56]. Ali et al. suggested a nine-layer textural CNN, achieving 90.69% accuracy [57]. Veasey et al. proposed a convolutional attention-based network using 2D feature extraction and achieved accuracy rates up to 88.1% [58]. Afshar et al. recommended a 3D multiscale capsule network, achieving 93.12% precision [59].

Overall, the CAD system for lung cancer detection encompasses ML-based, DL-based, image processing-based, and hybrid approaches. These studies have advanced the field of lung cancer diagnosis through various techniques and methodologies.

III. Classification Freamework For Lung Cancer

In this study, we introduce a unique hybrid deep learning model designed specifically for the diagnosis of lung cancer. We provide a comprehensive overview of its architecture, framework, and performance evaluation for classification. The entire classification process, as depicted in Figure 2, includes data collection, preprocessing, class labeling, model development, and evaluation.

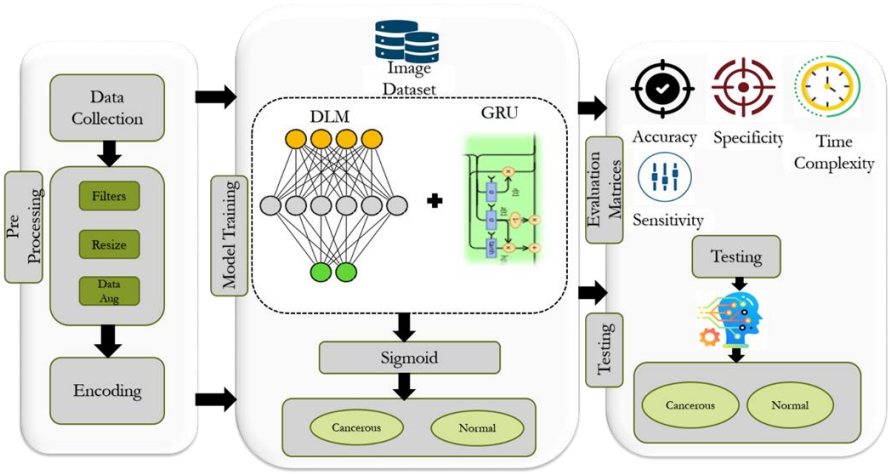

Figure 2: Block diagram of DenseNet201-GRU model for lung cancer classification

A. *Dataset Discrpation*

The lung CT scans utilized in this research can be accessed at https://wiki.cancerimagingarchive.net/display/Public/LIDC-IDRI. A total of 1018 lung CT scans from the National Cancer Institute were associated with experimental data from proteomics and genetics. In this section, we categorize all training radiographs into two groups: normal or showing malignant tumors. Nodules with a grade of 3 or below are considered normal, while those with a grade of 4 or above are classified as cancerous. Bronchial lesions with a malignancy score of 3 are excluded to prevent confusion. The NBIA retriever program is employed to retrieve DICOM image data from the tcia format, enabling its utilization in subsequent processing. Detailed descriptions of the testing datasets can be found on the tcia website [43].

B. *Data Preprocessing*

For obtaining accurate classification outcomes, preprocessing plays a vital role and is typically conducted on data prior to categorization. Preprocessing techniques are essential for enhancing the detection accuracy of the model on the "cancer dataset." Common preprocessing techniques utilized in lung cancer diagnosis include class labelling, image scaling, and data augmentation [44].

C. *Labeling of Clasess*

The lung cancer dataset undergoes a preprocessing step known as class labelling, where class labels are assigned to the data. In Figure 3, patients without cancer (Normal) are labelled as 0, while those with cancer are labelled as 1.

D. *Resizing*

In accordance with Figure 3, this study incorporates the resizing preprocessing technique. In order to ensure optimal training results, the proposed model necessitates images of consistent dimensions. Consequently, all photographs were uniformly resized to meet this requirments.

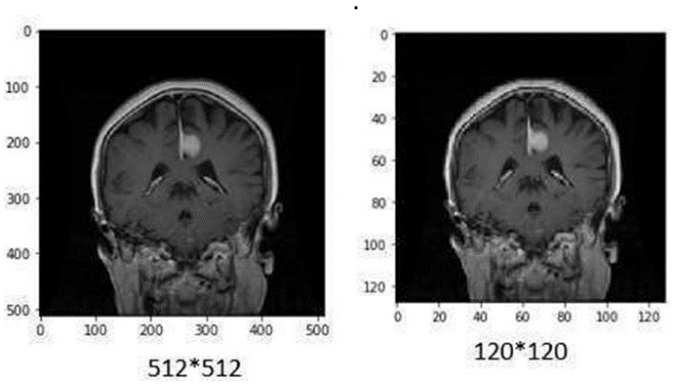

Figure 3: Resizing of CT images.

E. *Data Augmentation*

Data augmentation was applied to the cancer dataset. Convolutional neural networks (CNNs) generally benefit from large datasets to enhance performance; however, gathering such datasets can be challenging. Overfitting is a common concern with CNNs when data is limited, resulting in inaccurate performance evaluations of the models. To address this fundamental issue, data augmentation, as illustrated in Figure 4, is considered the most effective strategy.

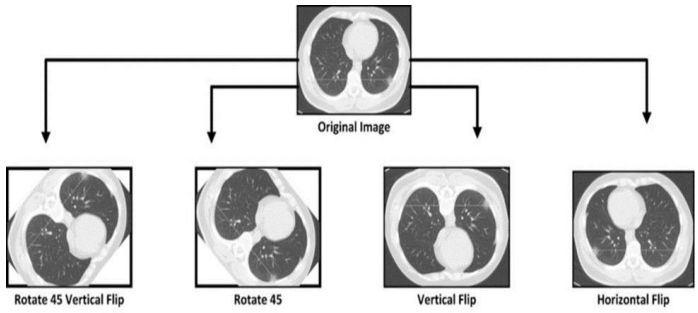

Figure 4: Augmentation of CT images

F. *Proposed System Model*

Once the data has undergone cleaning, transformation, and preparation, it will be input into the proposed model, namely

DenseNet201-GRU. This article focuses on exploring the DenseNet201 and GRU models, along with their respective training configurations, to effectively recognize and categorize lung cancer.

G. Densenet20

The DenseNet201 is a specific model within the convolutional neural network (CNN) family, known for its effectiveness in tasks like object detection, image categorization, and related domains. It incorporates key components such as maximum pooling of convolutions, ReLU activations, and dropout layers to enhance its performance and robustness.

H. Gated Recurrent Unit Network (GRU)

The GRU model is a popular choice in recurrent neural networks (RNNs) to address the challenge of vanishing gradients. Unlike the LSTM, GRU utilizes three main gates and an internal cell state, making it an efficient option. The GRU's gates securely store and manage information. The reset gate (r) enables the incorporation of current data, while the update gate (z) facilitates the inclusion of historical and future data. By storing data from the previous state, the reset gate enables seamless memory transfer. Additionally, the input's nonlinear modulation gate imparts the zero-mean properties of a nonlinear signal, enhancing its effectiveness.

I. Proposed Model: Densenet201-GRU

Our research suggests the utilization of the DenseNet201-GRU model for lung cancer classification as sown in Fig.5. The proposed model consists of seven convolutions, four max-pooling layers, three fully-connected layers, and employs the ReLU activation function. The model parameters and Dense-GRU architecture are depicted in the accompanying diagram. The input image, initially having a height of 60 RGB pixels, width of 60 pixels, and three channels (60, 60, 3), undergoes feature extraction through a single convolutional layer. This layer generates a feature map of size 128, using a kernel size of 1 and a stride of 3x3. The second layer employs Rectified Linear Units (ReLU) as the activation function to address dimensionality nonlinearity. The proposed structure includes a regular first layer and a third layer, with the 128 feature maps aligned to the input shape, defining the output shape of the first convolutional layer (60, 60). The pooling layer reduces the size of the training parameters to a maximum of (58, 58), allowing faster training of the model. After pooling, the parameters (58, 58, 128) pass through a dropout layer to prevent overfitting. A dropout rate of 0.9 is employed at the start of the convolution layer. Activation function (ReLU) and dropout layers are applied after each regular and max-pooling layer to further prevent overfitting. The flatten layer transforms the training parameters from size (42, 42) to a feature map of size (512), which is then fed into a fully connected layer. To address the issue of vanishing gradients, a GRU model with a fully connected layer of 1,024 neurons is incorporated. Two additional layers are intertwined with the GRU model. The final connected layer includes softmax functions for classification purposes. In conclusion, the DenseNet201-GRU model, consisting of convolutions, max-pooling, fully connected layers, and ReLU activation, is recommended for lung cancer classification based on our research findings.

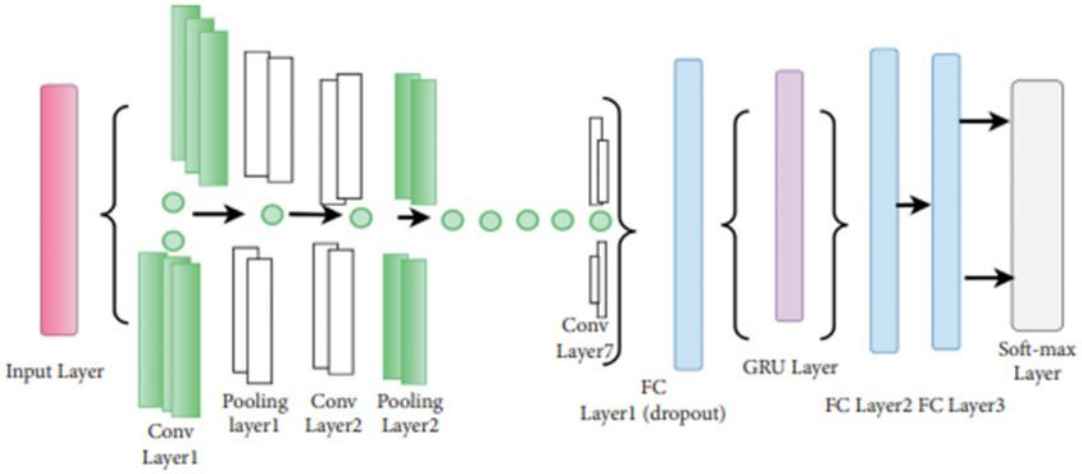

Figure 5: Structure Proposed DenseNet201-GRU model

IV. Results and Discussion

Detailed experimental setup and a thorough comparison of the suggested model 300 (DenseNet201-GRU) to the state-of-the-art ResNet50-GRU, ResNe50t-LSTM, and the most 301 current DL/ML models for lymph node lung cancer diagnosis are shown here.

A. *Performance Matrices*

The effectiveness of the model proposed is measured by its ability to accurately discriminate lung cancer (tumour) from normal tissue using many criteria:

TP: We got some bad news about the cancer samples.

FN: It is shorthand for "normal" (cancer-free) tissue samples.

FP: It seems bad but is likely to turn out okay.

FN: The model shows positive samples that are likely to be false.

Performance measurements for cancer diagnosis often include the following numerical representations of accuracy, precision, sensitivity, and specificity:

$$Accuracy = \frac{TN+TP}{TN+TP+FN+FP} x100\% \quad (1)$$

$$Specificity = \frac{TN \times 100\%}{TN+FP} x100\% \quad (2)$$

$$Sensitivity = \frac{TP}{TP+FN} x100\% \quad (3)$$

$$Precision = \frac{TP}{TP+FP} \text{x}100\% \quad (4)$$

B. *Accuracy, Specificty, Sensitivity & Precision*

In this study, the performance of three models, namely ResNet50-GRU, ResNet50-LSTM, and the recommended DenseNet201-GRU, was evaluated for the classification of cancer images.

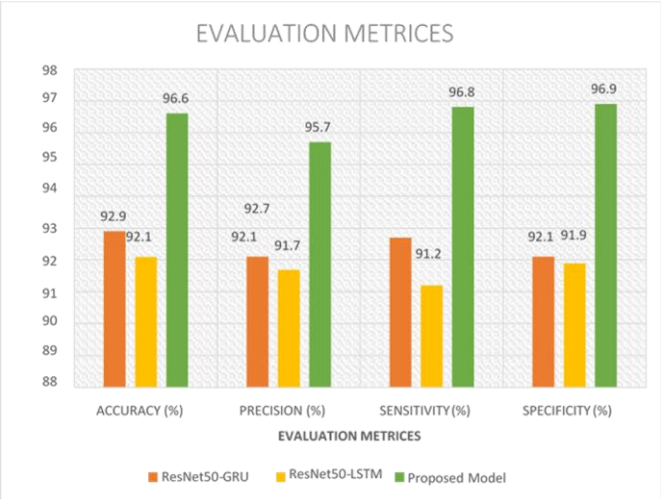

Figure 6: Comparative analysis of different hybrid models ResNet50-LSTM, ResNet50-GRU and Proposed model

Each model assigned only two potential values, 0 and 1. According to Fig. 6, the recommended model consistently outperformed ResNet50-GRU across all measured metrics, including specificity, accuracy, sensitivity, and precision. The experimental assessments of the models' precision, specificity, sensitivity, and accuracy are presented in the results.

C. *ROC: Reciver-Operating Characteristics Analysis*

In the evaluation of diagnostic tests, the area under the ROC curve (Receiver Operating Characteristic curve) is a valuable statistic that considers the trade-off between sensitivity and specificity. This statistic is particularly useful for assessing the effectiveness of tests in binary class identification, such as lung cancer detection.

In the case of lung cancer detection, the ROC curves of three models, namely DenseNet201-GRU, ResNet50-LSTM, and ResNet50-GRU, are depicted in Fig. 7, 8, 9. By comparing the ROC curves, it is evident that the proposed DenseNet201-GRU model accurately distinguishes between normal cancer and cancerous lymph nodes, surpassing the performance of ResNet50-LSTM and ResNet50-GRU models.

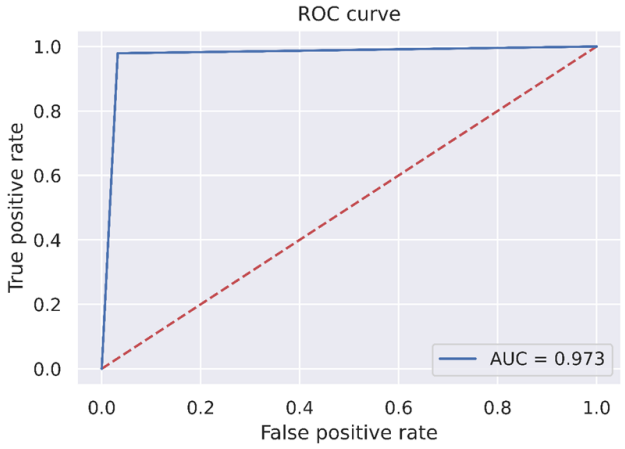

Figure 7: ROC Curve for the proposed DenseNet201-GRU Model

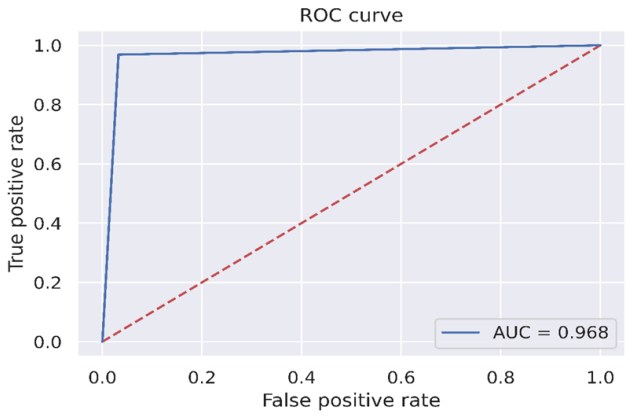

Figure 8: ROC Curve for ResNet50-GRU Model

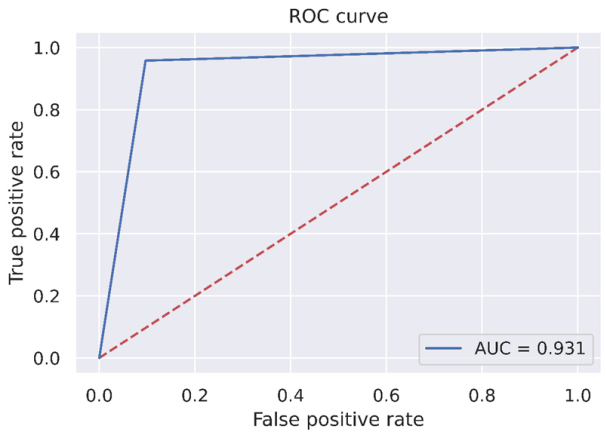

Figure 9: ROC Curve for ResNet50-LSTM Model

D. Time Complexity

The summarized outcomes of the tests on the models' temporal complexity are presented in the table below. It is worth noting that tracking progress during training can be challenging due to the lack of a controlled environment. Therefore, test results are considered a crucial metric for evaluating the efficacy and overall performance of the techniques. In the specific case of lung cancer detection, a binary class identification problem, the proposed DenseNet201-GRU model outperforms both the ResNet50-GRU and ResNet50-LSTM models. This phenomenon is depicted in Figure 14, which compares the proposed model with other popular deep learning algorithms used for binary tasks, such as CNNs, DNNs, LSTMs, GRUs, and bilinear neural networks. Notably, the DenseNet201-GRU model exhibits higher accuracy in percentage terms compared to the recommended models. However, it should be acknowledged that the suggested framework has a few limitations that require attention. To achieve faster training, the DenseNet-GRU approach requires substantial computing power and specialized hardware, such as a powerful graphics processing unit (GPU). Looking ahead, future healthcare systems can leverage other advanced AI technologies, including federated learning, deep learning, reinforcement learning, and deep reinforcement learning. Additionally, emerging sectors like Industry 4.0 and Industry 5.0 are expected to contribute significantly to the development of state-of-the-art medical equipment [59].

E. Confusion Matrix

To assess the classification performance of the implemented model, a confusion matrix was employed. The confusion matrix enables the classification of lung cancer into two categories: normal and cancerous. Specifically, the DenseNet-GRU model was evaluated using this classification measure and compared with the ResNet-LSTM and ResNet-GRU models. The results demonstrated that the DenseNet-GRU model outperformed the other hybrid models in accurately classifying lung cancer. This performance superiority is evident, which depict the comparison among the models. In conclusion, the utilization of a confusion matrix provided valuable insights into the classification performance of the models. The DenseNet-GRU model exhibited superior performance in accurately classifying lung cancer compared to the ResNet-LSTM and ResNet-GRU models.

CONCUSLION

The primary objective of this study is to utilize CT scans of the lung for the identification and categorization of cancerous cells compared to healthy ones. The automated detection and categorization of lung tissue areas in Whole Slide Images (WSIs) using a DenseNet201-GRU approach were explored. Early diagnosis plays a critical role in effective patient care, and automating tissue identification for lung cancer holds great potential but poses significant challenges. A model was developed in this study to aid in the diagnosis of lung cancer by automatically employing multiple layer topologies for IDC tissues. The efficacy of the proposed tumor detection method was evaluated using various performance metrics, including accuracy, f1-score, precision, recall, and specificity. The Tensorflow 1.8 tool with the Keras API was utilized for implementation. Based on the collected data, it is evident that the proposed architecture outperforms industry-standard architectures and achieves the highest performance levels. However, more extensive testing using larger real-time clinical datasets is required for further validation. The proposed model's results were compared to those of ResNet50-LSTM, ResNet50-GRU, and other existing ML/DL models. DenseNet201-GRU demonstrated higher precision, sensitivity, specificity, area under the curve, and F1-score, while also exhibiting lower time complexity (in milliseconds). Reducing the computational complexity of the suggested approach is essential to facilitate the accurate analysis and identification of tumor cells from the perspective of radiologists. Additionally, the proposed model holds potential for multiclass classification of lung cancer. In conclusion, this study presents a novel approach for automated detection and categorization of lung cancer cells using CT scans and a DenseNet201-GRU model. The achieved results surpass industry standards, showcasing the model's effectiveness in the diagnosis of lung cancer. Further advancements in testing and refinement are necessary, including the use of larger clinical datasets and addressing computational complexity.

REFERENCES

[1] World Health Organization. Available Online: https://www.who.int/news- room/fact-sheets/detail/cancer (accessed on 9 May 2022).

[2] Siegel, R.L.; Miller, K.D.; Fuchs, H.E.; Jemal, A. Cancer statistics, 2021. Cancer J. Clin. 2021, 71, 7–33. [CrossRef] [CrossRef] [PubMed]

[3] Wernick, M.N.; Yang, Y.; Brankov, J.G.; Yourganov, G.; Strother, S.C. Machine learning in medical imaging. IEEE Signal Process. Mag. 2010, 27, 25–38. [CrossRef] [CrossRef] [PubMed]

[4] De Bruijne M. Machine Learning Approaches in Medical Image Analysis: From Detection to Diagnosis. Med Image Anal (2016) 33:94–7. doi: 10.1016/j.media.2016.06.032 [PubMed] [CrossRef] [Google Scholar]

[5] Jindal A, Aujla GS, Kumar N, Chaudhary R, Obaidat MS, You I. Sedative: Sdn-Enabled Deep Learning Architecture for Network Traffic Control in Vehicular Cyber-Physical Systems. In: IEEE network; (2018). p. 66–73. [Google Scholar]

[6] Nalepa J, Kawulok M. Selecting Training Sets for Support Vector Machines: A Review. Artif Intell Rev (2019) 52:857–900. doi: 10.1007/s10462-017-9611-1 [CrossRef] [Google Scholar]

[7] Ganesan N, Venkatesh K, Rama M, Palani AM. Application of Neural Networks in Diagnosing Cancer Disease Using Demographic Data. Int J Comput Appl (2010) 1(26):76–85. doi: 10.5120/476-783 [CrossRef] [Google Scholar]

[8] Kasinathan G, Jayakumar S, Gandomi AH, Ramachandran M, Fong SJ, Patan R. Automated 3-D Lung Tumor Detection and Classification by an Active Contour Model and Cnn Classifier. Expert Syst Appl (2019) 134:112–9. doi: 10.1016/j.eswa.2019.05.041 [CrossRef] [Google Scholar]

[9] Shen D, Wu G, Suk HI. Deep Learning in Medical Image Analysis. Annu Rev Biomed Eng (2017) 19:221–48. doi: 10.1146/annurev-bioeng-071516-044442 [PMC free article] [PubMed] [CrossRef] [Google Scholar]

[10] Suzuki K. Overview of Deep Learning in Medical Imaging. Radiol Phys Technol (2017) 10(3):257–73. doi: Bharati S, Podder P, Mondal MRH. Hybrid Deep Learning for Detecting Lung Diseases From X-Ray Images. Inf Med Unlocked (2020) 20:100391. doi: 10.1016/j.imu.2020.100391 [PMC free article] [PubMed] [CrossRef] [Google Scholar]

[11] Tajbakhsh N, Suzuki K. Comparing Two Classes of End-to-End Machine-Learning Models in Lung Nodule Detection and Classification: Mtanns vs. Cnns. Pattern Recognit (2017) 63:476–86. doi: 10.1016/j.patcog.2016.09.029 [CrossRef] [Google Scholar]

[12] K. Nakamura, I. Jamil, X.L. Liu, O. Mitarai, M. Hasegawa, K. Tokunaga, K. Araki, H. Zushi, K. Hanada, A. Fujisawa, H. Idei, Y. Nagashima, S. Kawasaki, H. Nakashima and A. Higashijima, "Quaternion Analysis of Three-Phase Power Electronic Circuit by Using Conjugation, International Conference on Electrical Engineering", ICEE 2015, 15A-476 (2015).

[13] Sahu P, Yu D, Dasari M, Hou F, Qin H. A Lightweight Multi-Section Cnn for Lung Nodule Classification and Malignancy Estimation. IEEE J Biomed Health Inf (2018) 23(3):960–8. doi: 10.1109/JBHI.2018.2879834 [PubMed] [CrossRef] [Google Scholar]

[14] Bansal G, Chamola V, Narang P, Kumar S, Raman S. Deep3dscan: Deep Residual Network and Morphological Descriptor Based Framework for Lung Cancer Classification and 3d Segmentation. IET Imag Process (2020) 14(7):1240–7. doi: 10.1049/iet-ipr.2019.1164 [CrossRef] [Google Scholar]

[15] Jothi G, Inbarani HH. Soft Set Based Feature Selection Approach for Lung Cancer Images. ArXiv Preprint ArXiv (2012) 1212.5391. [Google Scholar]

[16] Anthimopoulos M, Christodoulidis S, Ebner L, Christe A, Mougiakakou S. Lung Pattern Classification for Interstitial Lung Diseases Using a Deep Convolutional Neural Network. IEEE Trans Med Imaging (2016) 35(5):1207–16. doi: 10.1109/TMI.2016.2535865 [PubMed] [CrossRef] [Google Scholar]

[17] Kasinathan G, Jayakumar S. Cloud-Based Lung Tumor Detection and Stage Classification Using Deep Learning Techniques. BioMed Res Int (2022) 2022:1–17. doi: 10.1155/2022/4185835 [PMC free article] [PubMed] [CrossRef] [Google Scholar]

[18] Jakimovski G, Davcev D. Using Double Convolution Neural Network for Lung Cancer Stage Detection. Appl Sci (2019) 9(3):427. doi: 10.3390/app9030427 [CrossRef] [Google Scholar]

[19] Yu H, Zhou Z, Wang Q. Deep Learning Assisted Predict of Lung Cancer on Computed Tomography Images Using the Adaptive Hierarchical Heuristic Mathematical Model. In: . IEEE Access; (2020). p. 86400–10. [Google Scholar]

[20] Jamil I., Lucheng H., Habib S., Aurangzeb M., Ahmed M. E, Jamil R., Performance evaluation of solar power plants for excess energy based on energy production, Volume 9, Pages 1501-1534, Energy Reports.

[21] Siegel, R.L.; Miller, K.D.; Jemal, A. Cancer statistics, 2015. CA Cancer J. Clin. 2015, 65, 5–29. [CrossRef] [PubMed]

[22] Usman M., Zhongjian D., Jamil I., Jamil R., Mubashir H. S., Model Building And Cascade Compensation Of Angle Servo Control System. Journal of Engineering Research and Application, Vol. 3, Issue 5, Sep-Oct 2013, pp.1000-1006.

[23] Baba, A.I.; Câtoi, C. Tumor cell morphology. In Comparative Oncology; The Publishing House of the Romanian Academy: Bucuresti, Romania, 2007.

[24] Wei, M.; Du, Y.; Wu, X.; Su, Q.; Zhu, J.; Zheng, L.; Lv, G.; Zhuang, J. A benign and malignant breast tumor classification method via efficiently combining texture and morphological features on ultrasound images. Comput. Wei, M.; Du, Y.; Wu, X.; Su, Q.; Zhu, J.; Zheng, L.; Lv, G.; Zhuang, J. A benign and malignant breast tumor classification method via efficiently combining texture and morphological features on ultrasound images. Comput. Math. Methods Med. 2020, 2020, 5894010. [CrossRef]

[25] Aurangzeb M., Jinquan Z., Jamil I, Ali. M. F, Case study of development boost converter with coupled inductors for PV system applications, 2016 IEEE 7th Annual Ubiquitous Computing, Electronics & Mobile Communication Conference (UEMCON), Pages 1-6, IEEE.

[26] Jia, T.; Zhang, H.; Bai, Y. Benign and malignant lung nodule classification based on deep learning feature. J. Med. Imaging Health Inform. 2015, 5, 1936–1940. [CrossRef]

[27] Snoeckx, A.; Reyntiens, P.; Desbuquoit, D.; Spinhoven, M.J.; Van Schil, P.E.; van Meerbeeck, J.P.; Parizel, P.M. Evaluation of the solitary pulmonary nodule: size matters, but do not ignore the power of morphology. Insights Imaging 2018, 9, 73– 86. [CrossRef] [PubMed]

[28] M. Fahad Ali, S. Linjun, I. Jamil, M. Aurangzeb, Research on Charging and Discharging of Lithium Ion Battery based on Temperature Controlled Technique, International Journal of Engineering Works, Vol. 6, Issue 05, PP. 153-158, May 2019.

[29] Jamil, I., Jamil, R., Jinquan, Z., Ming, L., Dong, W.Y. & Jamil, R. 2013. Condition-based maintenance decisionmaking support system (DSS) of hydropower plant. International Journal of Innovation and Applied Studies 4(3): 593–602.2170-2176 [CrossRef]

[30] Prokop, M.; Shin, H.O.; Schanz, A.; Schaefer-Prokop, C.M. Use of maximum intensity projections in CT angiography: A basic review. Radiographics 1997, 17, 433–451. [CrossRef]

[31] Afshar, P.; Oikonomou, A.; Naderkhani, F.; Tyrrell, P.N.; Plataniotis, K.N.; Farahani, K.; Mohammadi, A. 3D-MCN: A 3D multi-scale capsule network for lung nodule malignancy prediction. Sci. Rep. 2020, 10, 7948. [CrossRef]

[32] Li, Y.; Zhang, L.; Chen, H.; Yang, N. Lung nodule detection with deep learning in 3D thoracic MR images. IEEE Access 2019, 7, 37822–37832. [CrossRef]

[33] Dede, Y. Lung Cancer Dataset. 2018. Available online: https://www.kaggle.com/yusufdede/lung-cancer-dataset (accessed on 23 December 2021).

[34] Jamil I., Zhao J. and Jamil R., "Analysis, Design and Implementation of Zero-Current-Switching Resonant Converter DC-DC Buck Converter" International Journal of Electrical and Electronics Engineering (IJEEE) Vol. 2, Issue 2, May 2013741–749.

[35] Rustam, F.; Reshi, A.A.; Ashraf, I.; Mehmood, A.; Ullah, S.; Khan, D.M.; Choi, G.S. Sensor-based human activity recognition using deep stacked multilayered perceptron model. IEEE Access 2020, 8, 218898–218910. [CrossRef]

[36] Rupapara, V.; Rustam, F.; Shahzad, H.F.; Mehmood, A.; Ashraf, I.; Choi, G.S. Impact of SMOTE on imbalanced text features for toxic comments classification using RVVC model. IEEE Access 2021, 9, 78621–78634. [CrossRef]

[37] Jamil I., Jamil R., Jamil R., Jinquan Z. and Samee A., Technical Communication of Automation Control System in Water Treatment Plantl, International Journal of Innovative and Applied Studies, Vol. 4, No. 1. Sep. 2013, pp 28-36.

[38] Gaikwad, A.; Inamdar, A.; Behera, V. Lung cancer detection using digital Image processing on CT scan Images. Int. Res. J. Eng. Technol. (IRJET) IEEE e-ISSN 2016, 3, 2395–0056.

[39] Magdy, E.; Zayed, N.; Fakhr, M. Automatic classification of normal and cancer lung CT images using multiscale AM-FM features. Int. J. Biomed. Imaging 2015, 2015. [CrossRef]

[40] Jamil I. et al. "Matrix Converter in Power Electronics as a Power Supply for Plasma Control: A Short Review and a Foresight", Reports of Research Institute for Applied Mechanics, Kyushu University No.149 (24 – 29) September 2015.. [CrossRef]

[41] Shen, W.; Zhou, M.; Yang, F.; Yu, D.; Dong, D.; Yang, C.; Zang, Y.; Tian, J. Multi-crop convolutional neural networks for lung nodule malignancy suspiciousness classification. Pattern Recognit. 2017, 61, 663–673. [CrossRef]

[42] Chon, A.; Balachandar, N.; Lu, P. Deep Convolutional Neural Networks for Lung Cancer Detection; Standford University: Stanford, CA, USA, 2017; pp. 1–9.

[43] Ding, J.; Li, A.; Hu, Z.; Wang, L. Accurate pulmonary nodule detection in computed tomography images using deep convolutional neural networks. In International Conference on Medical Image Computing and Computer-Assisted Intervention; Springer: Cham, Switzerland, 2017; pp. 559–567.

[44] Zhu, W.; Liu, C.; Fan, W.; Xie, X. Deeplung: Deep 3d dual path nets for automated pulmonary nodule detection and classification. In Proceedings of the 2018 IEEE winter conference on Application of computer Vision(WACV), Lake Tahore, NV, USA, 12-15 March 2018; IEEE: Piscataway, NJ, USA, 2018; PP. 673-681

[45] To ˘gaçar, M.; Ergen, B.; Cömert, Z. Detection of lung cancer on chest CT images using minimum redundancy maximum relevance feature selection method with convolutional neural networks. Biocybern. Biomed. Eng. 2020, 40, 23–39. [CrossRef]

[46] Song, Q.; Zhao, L.; Luo, X.; Dou, X. Using deep learning for classification of lung nodules on computed tomography images. J. Healthc. Eng. 2017, 2017. [CrossRef]

[47] Jamil, I.; Zhao, J.; Zhang, L.; Jamil, R.; Rafique, S.F. Evaluation of Energy Production and Energy Yield Assessment Based on Feasibility, Design, and Execution of 3x50MW Grid-Connected Solar PV Pilot Project in Nooriabad. Int. J. Photoenergy 2017, 6429581. [CrossRef].

[48] Ali, I.; Muzammil, M.; Haq, I.U.; Khaliq, A.A.; Abdullah, S. Efficient lung nodule classification using transferable texture convolutional neural network. IEEE Access 2020, 8, 175859–175870. [CrossRef]

[49] Jamil, I.; Zhao, J.; Zhang, L.; Rafique, S.F.; Jamil, R. Uncertainty Analysis of Energy Production for a 3 50MW AC Photovoltaic Project Based on Solar Resources. Int. J. Photoenergy 2019, 2019, 1056735. [CrossRef] [PubMed]

[50] Tong, C.; Liang, B.; Su, Q.; Yu, M.; Hu, J.; Bashir, A.K.; Zheng, Z. Pulmonary nodule classification based on heterogeneous features learning. IEEE J. Sel. Areas Commun. 2020, 39, 574–581. [CrossRef]

[51] Forte, G.C.; Altmayer, S.; Silva, R.F.; Stefani, M.T.; Libermann, L.L.; Cavion, C.C.; Youssef, A.; Forghani, R.; King, J.; Mohamed, T.L.; et al. Deep Learning Algorithms for Diagnosis of Lung Cancer: A Systematic Review and Meta-Analysis. Cancers 2022, 14, 3856. [CrossRef] [PubMed]

[52] Fang, T. A novel computer-aided lung cancer detection method based on transfer learning from GoogLeNet and median intensity projections. In Proceedings of the 2018 IEEE International Conference on Computer and Communication Engineering Technology (CCET), Beijing, China, 18–20 August 2018; IEEE: Piscataway, NJ, USA, 2018; pp. 286–290.

[53] Jamil I., Jamil R., Jinquan Z., Ming L., Dong Y.W., and Jamil R., "Condition-Based Maintenance Decision-making Support System (DSS) of Hydropower Plant," Int. J. Innov. Appl. Stud., vol. 4, no. 3, pp. 593–602, Nov. 2013. 91–100.

[54] Hu, Q.; Whitney, H.M.; Li, H.; Ji, Y.; Liu, P.; Giger, M.L. Improved classification of benign and malignant breast lesions using deep feature maximum intensity projection MRI in breast cancer diagnosis using dynamic contrast-enhanced MRI. Radiol. Artif. Intell. 2021, 3, e200159. [CrossRef]

[55] Tariq, A.; Akram, M.U.; Javed, M.Y. Lung nodule detection in CT images using neuro fuzzy classifier. In Proceedings of the 2013 Fourth International Workshop on Computational Intelligence in Medical Imaging (CIMI), Singapore, 16–19 April 2013; IEEE: Piscataway, NJ, USA, 2013; pp. 49–53.

[56] Jamil I., Jamil R., Zhao J., Jamil R., and Abdus S., "Mathematical model analysis and control algorithms design based on state feedback method of rotary inverted pendulum," International Journal of Research in Engineering & Technology, vol. 1, no. 3, pp. 41–50, 2013

[57] Kumar, S.L.; Swathy, M.; Sathish, S.; Sivaraman, J.; Rajasekar, M. Identification of lung cancer cell using watershed segmentation on CT images. Indian J. Sci. Technol. 2016, 9, 1–4.

[58] Shakeel, P.M.; Burhanuddin, M.A.; Desa, M.I. Lung cancer detection from CT image using improved profuse clustering and deep learning instantaneously trained neural networks. Measurement 2019, 145, 702–712. [CrossRef]

[59] Matsumoto, S.; Kundel, H.L.; Gee, J.C.; Gefter, W.B.; Hatabu, H. Pulmonary nodule detection in CT images with quantized convergence index filter. Med. Image Anal. 2006, 10, 343–352. [CrossRef]

How to cite this article:

Abdul Jabbar, M. Irfan Khtaak, Arif ULLAH "Using Computer Tomographic (CT) Images, A Rebust Hybrid Computer-Aided Deep Learning Framework for Lung Cancer Classification" International Journal of Engineering Works, Vol. 10, Issue 06, PP. 55-63, June 2023. https://doi.org/10.34259/ijew.23.10065563.